PALEO-POLE POSITIONS FROM MARTIAN MAGNETIC ANOMALY DATA

Patrick T.Taylor

Geodynamics Branch

NASA/Goddard Space Flight Center

Greenbelt,MD

(301)614-5214

Fax (301)614-6522

ptaylor@ltpmail.gsfc.nasa.gov

James J. Frawley

Herring Bay Geophysics

440 Fairhaven Road

Tracys Landing,MD20779

(301)855-6169

hbgjjf@ltpmailx.gsfc.nasa.gov

27 Pages, 5 Figures,2 tables

– Running Heading: Martian Paleopoles

contact: James J. Frawley

440 Fairhaven Road

Tracys Landing.MD20754

(301)855-6169

– ***hbgjjf@ltpmailx.gsfc.nasa.gov***

Abstract

Magnetic component anomaly maps were made from five mapping cycles of the Mars Global Surveyor's magnetometer data. Our goal was to find and isolate positive and negative anomaly pairs which would indicate magnetization of a single source body. From these anomalies we could compute the direction of the magnetizing vector and subsequently the location of the magnetic pole existing at the time of magnetization. We found nine suitable anomaly pairs and from these we computed four North and 3 South poles with two at approximately 60 degrees north latitude. These results suggest that during the existence of the Martian main magnetic field it experienced several reversals.

– **Key words:** Mars, Data Reduction Techniques, Geophysics, Magnetic Fields.

– Introduction

The Mars Global Surveyor (MGS) was launched from the NASA Kennedy Space Center, Florida on November 7, 1996 and arrived at Mars some ten months later. Orbital insertion began on September 11, 1997 and the Science Phasing Orbits (SPO) took place between May and November, 1998 while the missions mapping phase began in March, 1999. A magnetometer and electron reflectometer (MAG/ER) were part of the instrument payload. A triaxial fluxgate magnetometer records three mutually orthogonal field components, a further description of these instruments can be found in Acuna et al. (1998) and the references therein. The first magnetic anomaly maps of the Martian field (Acuna et al., 1999, Ness et al., 2000, Purucker et al., 2000 and Connerney et al., 2001) revealed that Mars lacks a dipole or main magnetic field but that there were many large amplitude magnetic anomalies. Most of these were located in the southern highlands and uncorrelated with either topography or the large impact basins. They had to have been produced by remanent magnetization, a process where the rock records and remembers the magnetizing field even after it is removed (Ness et al., 1999)an idea which had been earlier proposed by Curtis and Ness (1988) and Lewelling and Spohn (1997). There have been several interpretations on a planetary scale of the geological significance of these crustal anomalies (Connerney et al, 1999 and 2001; Arkani-Hamed, 2001 and 2002; and Purucker et al., 2000). Connerney et al. (1999) interpreted these anomalies as indicating a former period of plate tectonics. This hypothesis has been discussed by others (Harrison, 2000, Connerney et al., 2000 and Nimmo, 2000). In this study, however, we will focus on the single source isolated anomalies that are characterized by distinct dipole (positive and negative) anomalies. Our objective is to select those isolated anomalies that exhibit properties of being produced by a single uniformly magnetized source and we have fitted a magnetization vector from where we

could determine the location of the magnetizing pole. Similar studies have been done by Hood and Zakharian (2001) and Arkani-Hamed (2001 and 2002). We selected nine of these distinct anomalies from the Martian crustal field. There are more of these isolated anomalies in the Martian field than on Earth (Langel and Hinze, 1998) since the latter are often formed by proximal sources that produce overlapping fields that give variable directions and intensities. This report described our data analysis method and how the selected isolated magnetic anomalies were used to derive these paleo-pole positions.

Data from the magnetometer/electron reflectometer (MAG/ER) experiment aboard the MGS (Acuna et al., 1998) was obtained from the Institute of Geophysics and Planetary Physics, Planetary Data System at the University of California, Los Angeles for the periods covering the aero-braking phase, Science Phasing Orbits 1 and 2 and the mapping mission from March, 1999 to August, 1999, or approximately five mapping cycles (28 days/cycle) were used in our study. These data were contained on twenty-four CD-ROMs and included processed orbit information as well as the Magnetic and Electron Reflectometer Experiment results. In addition to MAG/ER observations, magnetic compensation fields and spacecraft currents for each observation were recorded. The magnetic compensation fields included both static and dynamic terms for each axis. The rms field of each axis was also recorded to aid in the detection of external field and instrument noise.

– Data Processing

Initially, global maps of the Martian magnetic anomalies were produced using night-side passes acquired from 3/8/99 to 5/4/99. This was done to avoid the Martian magnetosphere produced by solar radiation. Data were selected between 87°N and 87°S. Each magnetic component (x, north-south; y, east-west; z, vertical) was de-trended with a second-order-Fourier series, and the selected passes were screened manually for external field effects. After a relatively clean set of passes were obtained, they were binned at a one-degree grid interval. The global maps for total field and three components are shown in Fig. 1. Visual inspection of these maps at once showed two things: a) the Martian crustal magnetic field, like the topography, is dichotomous; and b) a number of the anomalies were isolated and could be modeled as being produced from the magnetization of a single isolated body. These aspects of the Martian magnetic anomaly field have been noted by other investigators (Acuna et al., (1999), Arkani-Ahmed (2001 and 2002), Hood and Zakharian (2001), Purucker et al.(2000)) and others. The dichotomous crustal field does not correlate with the topography accept only in the most general sense; the region of high magnetization occurs in the southern hemisphere and is generally centered longitudinally on the southern-cratered highlands. Using these global maps, a number of areas were selected for more detailed analysis. These were all regions where there were isolated anomalies, with the exception of the region of high magnetization (RHM), which was analyzed separately. Figure 2 shows the locations of seven of the eight sub-areas, each of which was in turn sub-divided into regions where the individual isolated anomalies occurred.

Production of final contour maps for selected regions of the planet mars took place in eight steps:

[1.] Extract data selected for each chosen area from the sixteen mapping phase CD-ROMs ,rotate into planetary coordinates and concatenate. Sort and number tracks as ascending or descending and plot on map projection. De-trend tracks with a first-order polynomial. Grid descending tracks at 40 km interval using minimum curvature/Akima interpolator

algorithms. Sort descending tracks used to make initial grid by longitude and plot F (scalar field), X, Y and Z in groups of five. Each group of five was then screened manually for external noise, i.e., non-crustal fields. Generate a new selection of descending orbits excluding bad or noisy tracks. Re-grid tracks using culled data set. Low-pass filter gridded data using 0.1 -0 .25 /data interval cutoff .

This process was done separately for the each of the total field and X, Y and Z components. After viewing profiles from several full orbits it was decided to use only the more noise free descending or nighttime passes in making the magnetic maps. This is because the MGS is in a sun-synchronous orbit, crossing the equator at 2 pm local on the ascending pass and 2 am local on the descending pass. Thus, the descending passes suffered less from external fields and gave a better representation of the crustal fields (Ness et al., 2000). A first order polynomial was used to de-trend each track after trying polynomials of orders 0 through 4. The first order polynomial seemed to give the best match of adjacent profiles and did not introduce any artificial frequencies into the data. Figure 3 shows a sample of profiles of adjacent tracks .

There were generally about 300 tracks in each 60 x 60 degree area. After eliminating tracks with high noise/external field levels, there were usually about 250 useable tracks remaining. Figure 4 is an example of the data from one of our study areas, number 3, and shows all the tracks used in making the final smoothed contour map.

5. Analysis

Final contours for the X, Y and Z components for each of the areas are shown in Fig. 5 (a-g). All the isolated anomalies displayed the classic morphologies of an isolated source. The relative positions of the highs and lows for each component gave an indication of the direction of magnetization, and the spacing between the highs and lows an indication of depth to source (Blakely, 1995).

All of our magnetic anomaly locations are in the Martian highlands and all but two are located in the southern hemisphere (Fig. 2). One isolated anomaly occurs in Area 2 (Table 1 and Fig. 2) on the southern edge of Claritis Rupes , the western border of Syria Planum, however there is no significant correlation between this anomaly and any distinct physiographic feature. Area 3 partially overlaps the western most section of Area 2. There were three isolated anomaly pairs selected from this region. The eastern most of these anomalies lies at the extreme base of Arisa Mons on Daedalia Planum with the vertical component coincident with the small crater Amazonis Sulci, however, this crater is small and may or may not be related to the anomaly. The other two isolated anomalies we selected from this area are between the craters Marca and Burton and Comas Sola and Bernard. However, the western half of Area 3 is heavily cratered, and any anomaly in this area would lie on or near a crater. It must be mentioned again that our criteron for anomaly selection is based on choosing isolated anomalies with developed single source features, that is, a distinct or recognizable positive and negative doublet anomaly pair and not on the largest amplitude features. Three isolated anomalies were analyzed

from Area 4. This region is dominated by the Valles Marinaris and the northern half of Argyre Planitia, however, one anomaly lies to the north and the others further to the south of this feature. The northernmost anomaly is on the Ophir Planum, just west of the Ganges Chasm, on the southwestern boundary of the larger Xanthe Terra. With one between the Noachis Terra and Bosporus Planum near the crater Bunge. The southernmost anomaly lies to the southwest on the Bosporus Planum, neither of these are correlated with distinct topographic features. The last two selected anomalies, from Area 8 , one near Ares Valles on Arabia Terra and the other on the southern border of Arcadia Planitia.

– Crustal Anomaly Maps

Using the processing procedures previosuly described, magnetic anomaly maps were generated for seven 60 x 60 degree regions. All the areas except one covered the latitude band 50°S-10°N. The extent of areas 2-8 is listed in Table 1 and shown in Fig. 2.

Area #	Lat Range	Lon Range
2	50S-10N	75W-135W
3	50S-10N	180W-120W
4	50S-10N	90W-30W
5	50S-10N	30W-30E
6	50S-10N	30E-90E
7	50S-10N	90E-150E
8	30S-30N	30W-30E

Table I Test Area Limits

The most striking features to be seen with the generation of the first component maps were the existence of well defined, isolated magnetic sources. These showed a classic distribution of maxima and minima in each component indicative of a single source with a constant direction of magnetization. Since present day Mars has no discernable core field, the formation of these sources are the result of remanence, that is, magnetization occured in the past when Mars had a main or core field similar to the present day of the Earth (Zatman et al., 2001). Accordingly, each individual area map was examined for isolated magnetic sources and each was marked for further analysis. Other areas were not used either because they did not have any good single source anomalies or because, as in area 7, the field was much more complex. Several methods were applied to these anomalies to derive a direction of magnetization. One of the inverse methods tested was Parkers determination from X, Y and Z com-

ponents (Parker et al., 1987), originally developed to estimate the magnetization of seamounts (many of which are often text-book examples of isolated anomalies). This was found to be far too sensitive to position and size of the data grid to be of use. A second inverse method tested involved Helbig's (Helbig, 1963) use of moments of the components for magnetization directions. This proved to be less satisfactory than the first in terms of variability and sensitivity to position and areal extent of the measured data. Even though it had been used successfully in the past to determine direction of magnetization from Magsat data over the Kursk Magnetic Anomaly, Russia (Taylor and Frawley, 1987) it did not seem to work well with the Martian anomalies. Finally, several forward modeling schemes were used to simulate the measured fields. These included magnetic polygonal prisms and simple dipole sources. The dipole source was settled on as a limiting case. For most of the single source anomalies these methods could reproduce the maxima and minima and their spacing well enough to get a direction of magnetization that was consistent with the vector geometry. They also represented a maximum magnetization and a minimum depth for the source. In only one of the cases was the spacing of the maxima and minima wide enough in the Y component to suggest that the source has some areal extent broader than a single point. Thus, using forward modeling with dipoles, it was possible to determine the direction of magnetization for 9 of the single source anomalies. See Fig. 5 for an example of how the dipole fields compared to the measured fields With these magnetization directions, it was then possible to estimate the location of the paleo-poles, given the location of the anomalies shown in Table II.

Area	#	Lat	Lon	Depth (km)	Moment $10^{16}A\text{-}m^2$	Dip	Dec	Paleolat	Paleolon
2	1	28S	105W	40	1.32	-45	0	88.6N	105W
3	2	7S	144W	40	2.9	-45	0	70.4N	36E
3	3	16S	165W	80	5.29	-34	0	87.4N	15E
3	4	35S	165W	200	9.9	-50	0	85.7N	165W
4	5	8S	54W	40	2.9	0	180	82S	126E
4	6	32S	47W	160	5.29	0	0	58N	47W
4	7	38S	65W	160	4.23	-10	180	57N	65W
8	8	4N	17W	20	2.18	0	180	86S	17W
8	9	1N	0	20	2.18	0	180	89S	0

Table II

– Discussion and Conclusion

Several crustal magnetic anomalies have been defined from the MGS MAG/ER data. Paleo-poles computed from these may suggest that Mars original magnetic field was at times reversed similar to that of the Earth's field. The fact that the declinations of the anomalies examined were all near zero or 180 degrees indicates that at the time their remenant magnetization was acquired the direction of the Martian main field must have been close to the planets' present day axis of rotation. It is not possible at this point to determine when the Martian main field disappeared, nor how long it was in existence.

Hood and Zakharian (2001) conducted a similar study on two isolated magnetic anomalies in the Martian northern polar region ((83°N, 32°E and 65°N, 27°E). They found that the pole positions for these anomalies were situated in an area north of Olympus Mons (50°N, 135°W). Likewise, Arkani-Hamed (2001) computed pole positions for ten small isolated magnetic anomalies in both hemispheres and ranging from 65°N to 27°S latitude. He found that seven of the ten computed poles were distributed within thirty degrees of the point at 25°N latitude, 230°E longitude. Two of our anomalies are located near those studied by Arkani-Hamed (2001); our numbers 2 and 8 correspond with M7 and M10 of Arkani-Hamed (2001) respectively. The results differ significantly (our 2 and M7-paleo-latitude: 70 N versus 35 S and paleo-longitude: 36 E versus 40 E and for 8 and M10 (paleo-latitude: 86S versus 4N and paleo-longitude 17W versus 168E). Arkani-Hamed (2001) fitted a vector of magnetization to a vertical prism with an elliptical cross section whose top was the Martian surface while we fitted a vector dipole to the anomaly field itself; similar to the procedure practiced in determining the paleo-pole from seamount data (e.g., Mayhew, 1986). Some of these discrepencies may be accounted for by the different techniques used to isolate the anomalies. However, in the case of the second example, the discrepancy can be explained by what part of the field is considered as arising from a single source. In our case we considered the high-low pair in the Z component, for example, to be generated by a single horizontally polarized source, whereas Arkani-Hamed's model assumes the Z component is one lobed, resulting in a vertically polarized source (implying that the source of the adjacent lobe is radially polarized in the reverse direction). In the first case it should be noted that the two directions of magnetization are simialr in dip (45S vs 66S) but approximately 180 out in declination(0 vs 172W) Plots of the potential and component fields produced by sources with these two magnetzations show that they are similar in the main features.

Interpretations of satellite altitude anomalies on the Earth are greatly aided by the large amount of geologic, ground-based geophysical and tectonic data (see, Langel and Hinze, 1998). This geologic information is used to define and constrain the interpretations of the Earth-orbiting magnetic satellite missions, unfortunately, a similar set of data is not available for Mars. In order to begin to make geologically resonable interpretations we should, at least, know the thickness and structure of the crust and have a quasi-planetary sampling of the petromagnetic and paleomagnetic properties of the crust; until these data are available we will have divergent views for the interpretation of the Martian magnetic field.

Acknowledgments

This work was done under NASA Headquarters Grant Number NAG5-9832.

REFERENCES

Acuña, M. H. and others 1998. Magnetic Field and Plasma Observations at Mars: Initial Results of the Mars Global Survey Mission. Science ***279,*** *1676-1680.*

Acuña, M. H. and others 1999. Global Distribution of Crustal Magnetization Discovered by the Mars Global Survey MAG/ER Experimetn. Science ***284****, 790-793.*

Arkani-Hamed, J. 2002. Magnetization of the Martian crust. Journal of Geophysical Research ***107****, 8-1-8-10.*

Arkani-Hamed, J.2001. Paleomagnetic Pole Positions and Pole Reversals of Mars. Geophysical Research Letters ***28****, 3409-3412.*

Blakeley, R.J. 1995. Potential Theory in Gravity & Magnetic Applications, Cambridge University Press, Cambridge.

Connerney, J.E. and other 2001. The Global Magnetic Field of Mars and Implications for Crustal Evolution. Geophysical Research Letters ***28****, 4015-4018.*

Connerney, J.E. and others 1999. Magnetic Lineations in the Ancient Crust of Mars Science ***284****, 794-798.*

Connerney, J.E. and others 2000. Response. Science ***287****, 548.*

Curtis, S.A. and N.F. Ness 1988. Remanent Magnetism at Mars. Geophysical Research Letters ***15****, 737-739.*

Harrison, C.G.A., 20002. Questions About Magnetic Lineations in the Ancient Crust of Mars, Science ***287****, 547.*

Hood, L.L. and A. Zakharian 2001. Mapping and modeling of magnetic anomalies in the northern polar region of Mars. Journal of Geophysical Research ***106****, 14,601-14,619.*

Langel, R.A. and W.J. Hinze 1998. The Magnetic Field of the Earth's Lithosphere: The Satellite Perspective, Cambridge University Press, Cambridge.

Leweling M. and T. Spohn 1997. Mars: a magnetic field due to thermoremanence? Planetary and Space Science ***45****, 1389-1400.*

Mayhew, M.A. 1986. Approximate paleomagnetic poles for some of the New England Seamounts. Earth

and Planetary Science Letters **79**, *185-194.*

Ness, N.F. and others 1999. MGS Magnetic Fields and Electron Reflectometer Investigation: Discovery of paleomagnetic Fields Due to Crustal Remanence. Advances in Space Research **23**, *1879-1886.*

Ness, N.F. and others 2000. Effects of magnetic anomalies discovered at Mars on the structure of the Martian ionosphere and solar wind interaction as follows from radio occultation experiments. Journal of Geophysical Research **105**, *15991-16004.*

Nimmo, F., 2000. Dike intrusion as a possible cause of linear Martian magnetic anomalies. Geology **28**, *391-394.*

Parker, R.L., L. Shure and J.A. Hildenbrand 1987. The application of inverse theory to seamount magnetism. Reviews of Geophysics **25**, *17-40.*

Purucker, M. and others 2000. An altitude-normalized magnetic map of Mars and its interpretation. Geophysical Research Letters **27**, *2449-2452.*

Zatman, S. D. Stegman, D. Ravat, P. Taylor and J. Frawley 2001. Geodynamic constraints on the age of the Martian magnetic anomaly construction. EOS Transactions AGU **82 (20)**, *S127.*

•

TABLE I

Area #	Lat Range	Lon Range
1	50S-10N	75W-135W
2	50S-10N	180W-120W
3	50S-10N	90W-30W
4	50S-10N	30W-30E
5	50S-10N	30E-90E
6	50S-10N	90E-150E
7	30S-30N	30W-30E

Table 1

Test Area Limits

• Table II

Area	#	Lat	Lon	Depth (km)	Moment $10^{16}A\text{-}m^2$	Dip	Dec	Paleo lat	Paleo lon
2	1	28S	105W	40	1.32	-45	0	88.6N	105W
3	2	7S	144W	40	2.9	-45	0	70.4N	36E
3	3	16S	165W	80	5.29	-34	0	87.4N	15E
3	4	35S	165W	200	9.9	-50	0	85.7N	165W
4	5	8S	54W	40	2.9	0	180	82S	126E
4	6	32S	47W	160	5.29	0	0	58N	47W
4	7	38S	65W	160	4.23	-10	180	57N	65W
8	8	4N	17W	20	2.18	0	180	86S	17W
8	9	1N	0	20	2.18	0	180	89S	0

Table II

Figures:

1. Global maps for X (North),Y (East) and Z (Vertical) components.
2. Locations of seven sub-areas where isolated anomalies were located with selected geographic.
3. Samples of selected profiles of five adjacent MGS tracks, Total Field, X, Y and Z.
4. Example of track coverage for Area 3. Other areas display a similar high density of orbits.

5 a-g. Component contours for areas and dipole fit to the anomaly fields. Contour intervals vary and are given for each area.

6. Anomaly-Paleopole positions, X represents location of the paleopole triangles indicate anomaly location.

MARS **Crustal Anomaly Field at 400km - X Component**

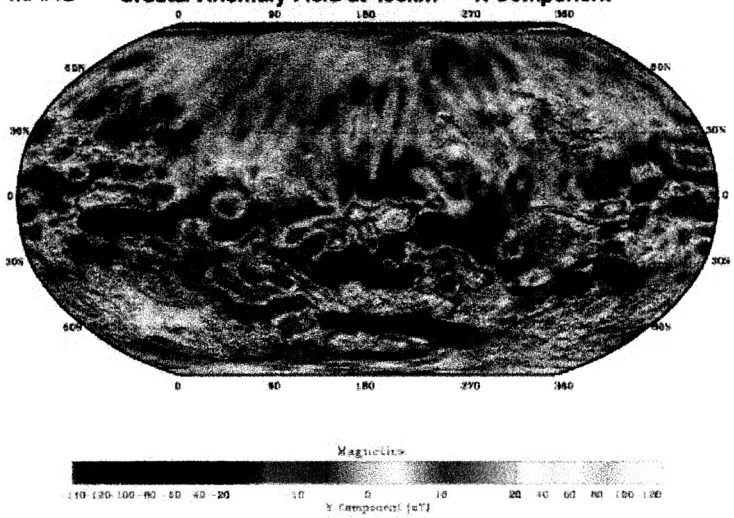

Crustal Anomaly Field at 400km - Y Component

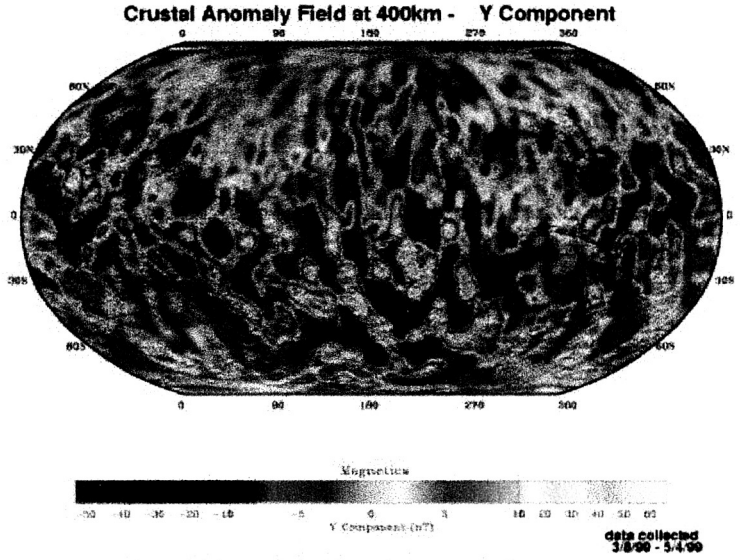

Crustal Anomaly Field at 400km - Z Component

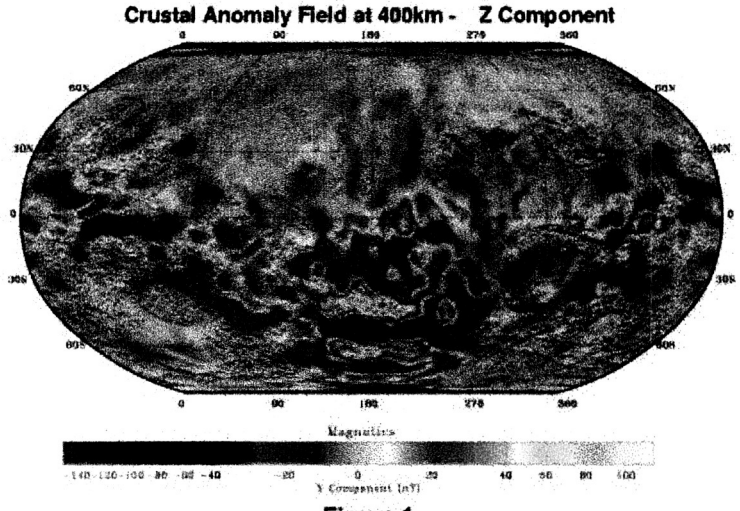

Figure 1

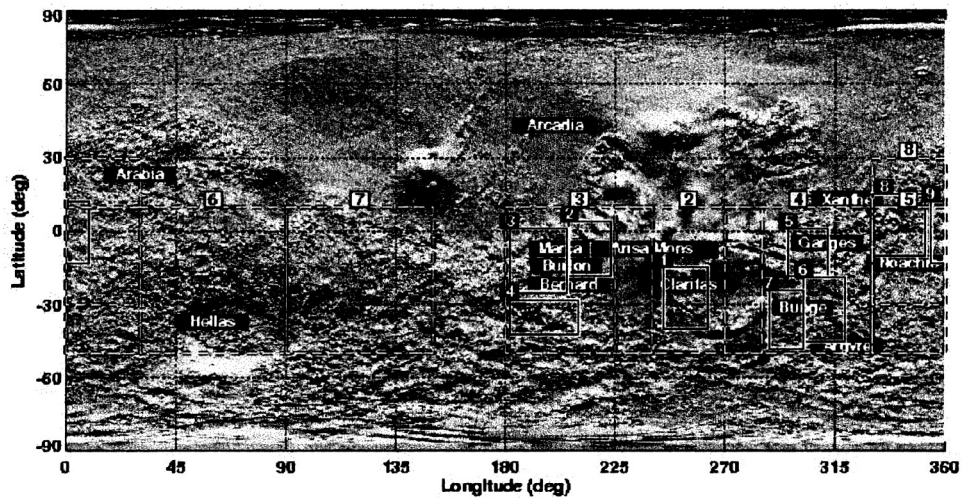

Figure 2
Study Area and Anomaly Locations

Figure 2
Figure 3

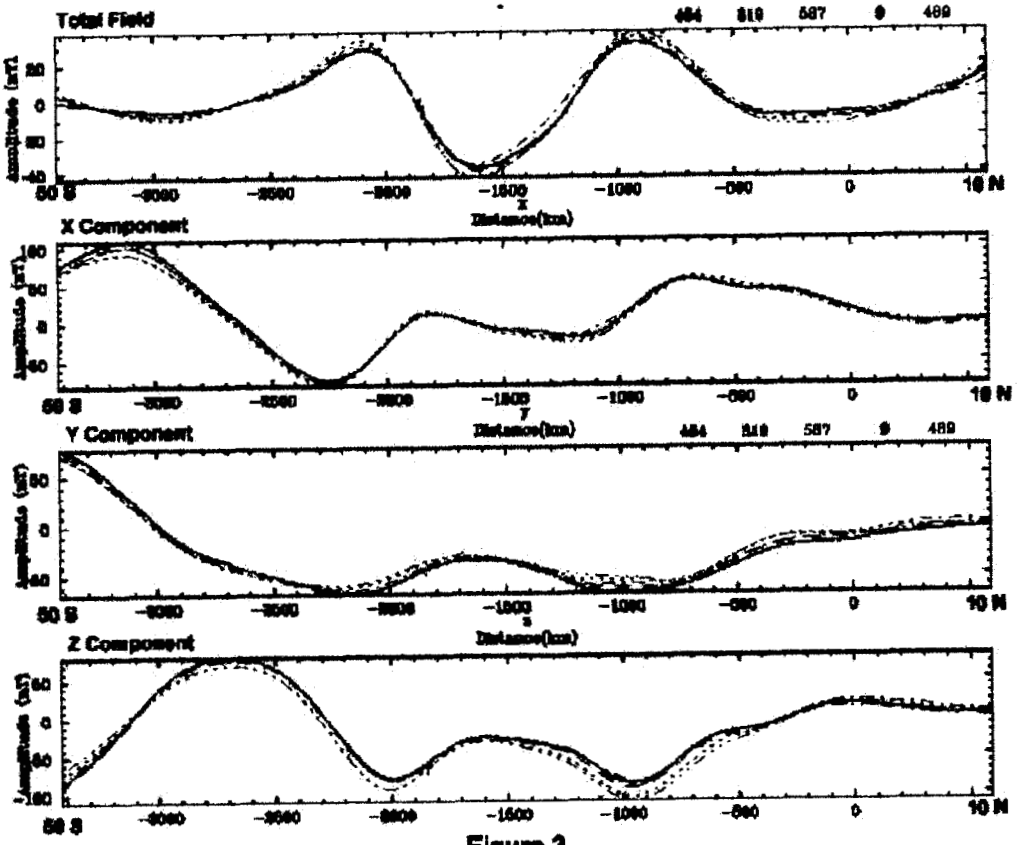

Figure 3
Five Adjacent Tracks in Area 4

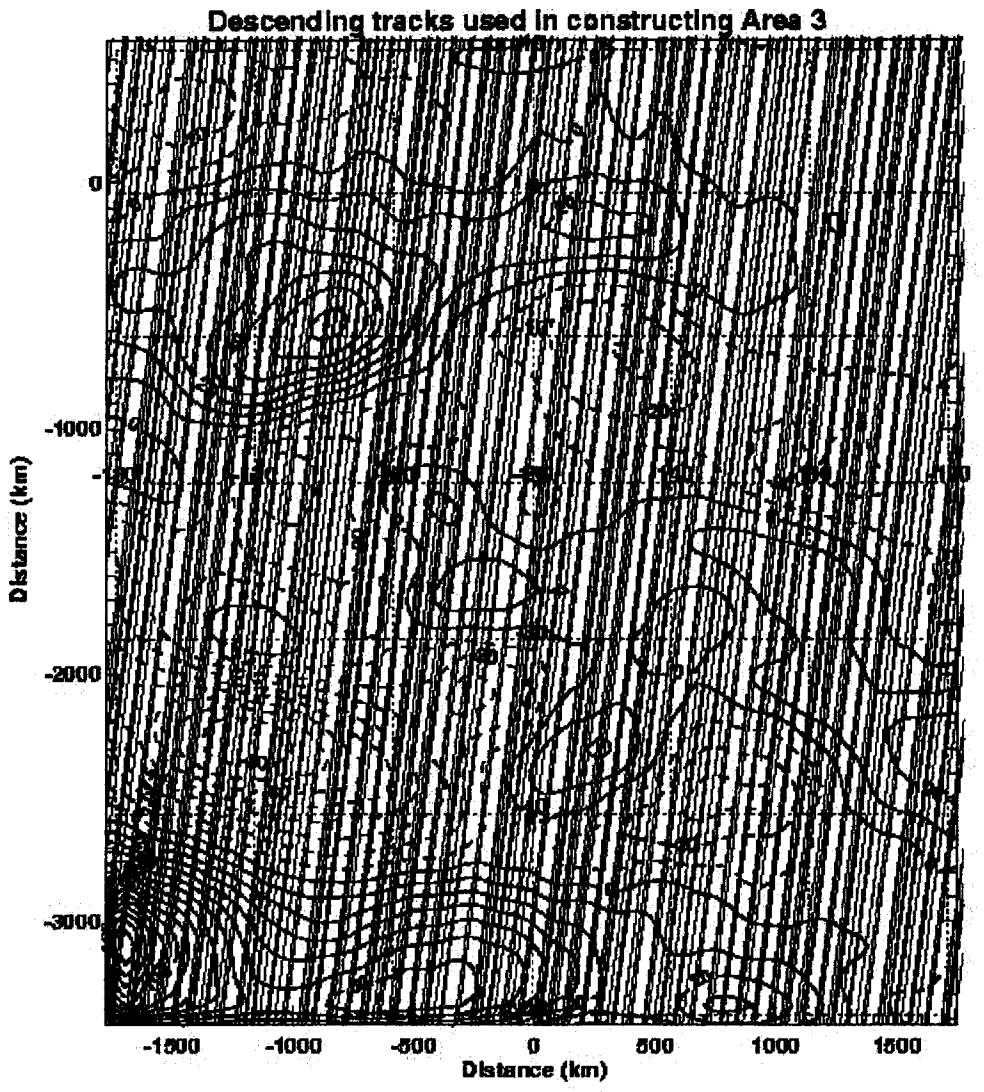

Figure 4 - X Component

Mon Aug 4 13:04:52 2003

c.I.=10 nT

figure 4

figure 5a

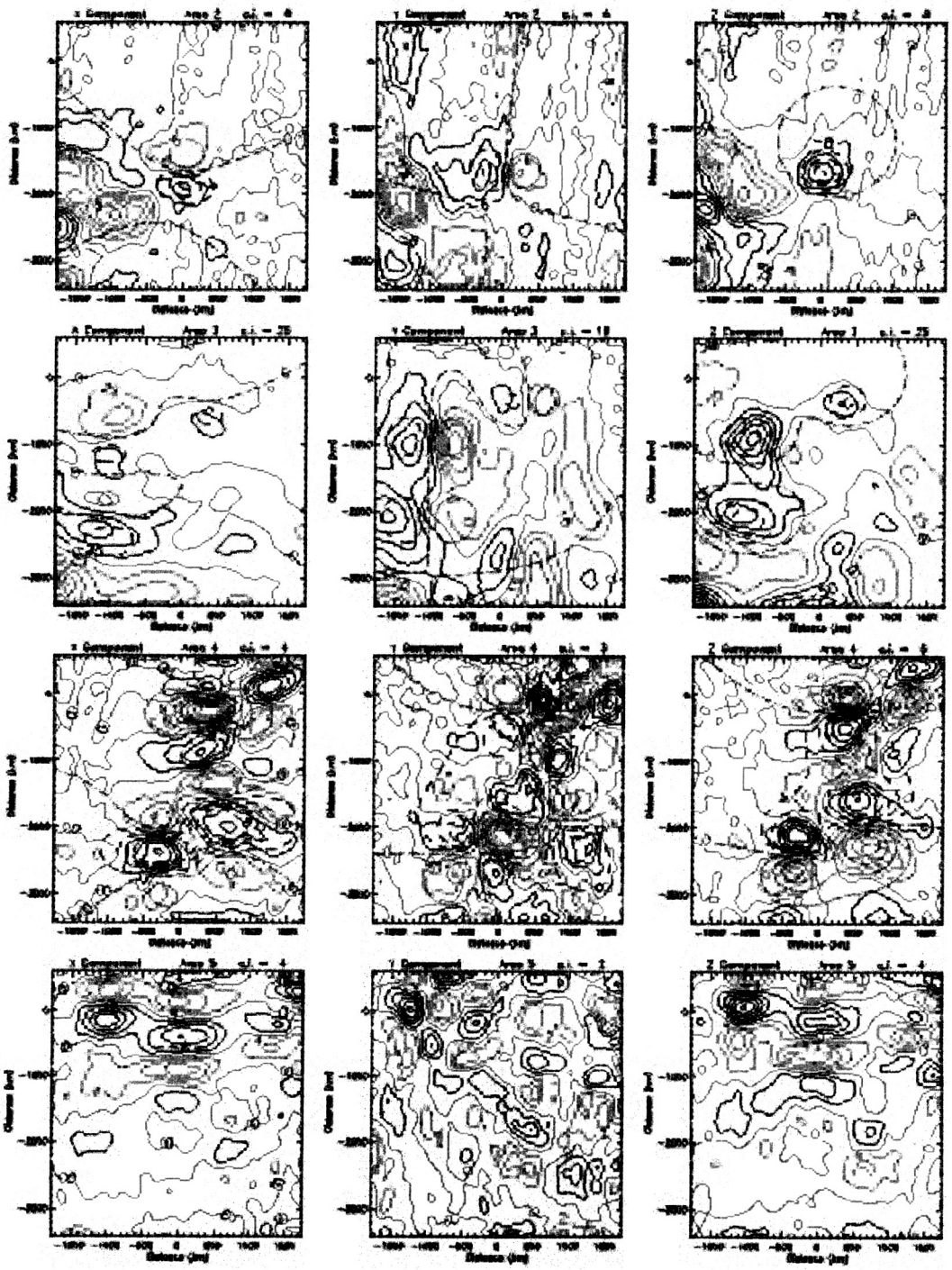

figure 5b

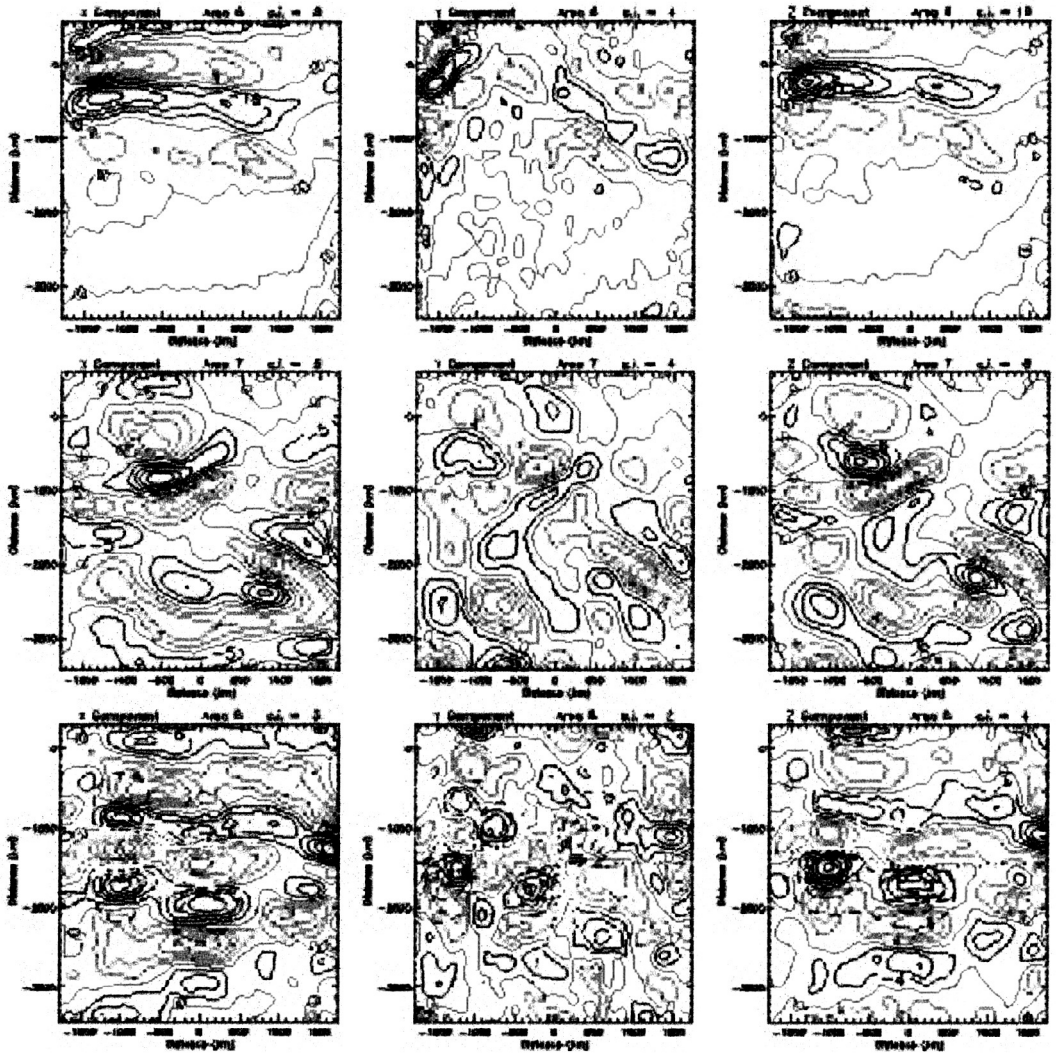

Figure 5

Contours for areas 2-8 with dipole model superimposed

Figure 6

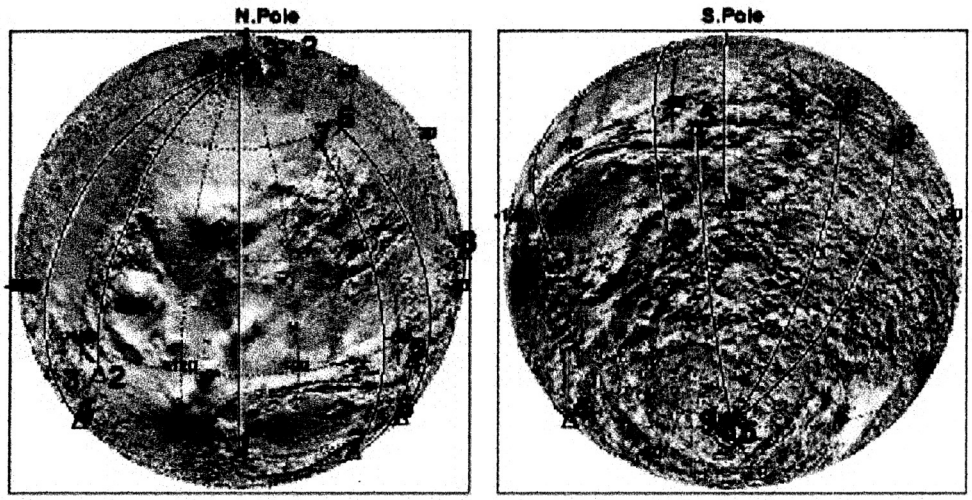

Figure 6
Anamoly and Paleopole locations on Topography

1